

# Non-diffusive Numerical Scheme for Regularized Mean Curvature Flow Level Set Equation in Image Processing

Robert Eymard  
Université Paris-Est,  
France

Angela Handlovičová  
Slovak University of Technology Bratislava,  
Slovakia

Karol Mikula  
Slovak University of Technology Bratislava,  
Slovakia

**Abstract**—We present new numerical scheme for solving regularised mean curvature flow level set equation and show its behavior in image filtering examples. The scheme is based on finite volume space discretization and semi-implicit time discretization [9], it is unconditionally stable and very weakly diffusive. Such properties are important in image filtering where they guarantee correct reconstruction of shapes deteriorated by high level of noise in stable and computationally efficient way. We compare the filtering capabilities of our new scheme with the standard explicit finite difference approximation of the mean curvature level set equation [15] and show appropriate behavior of the new method.

## I. LEVEL SET FORMULATION OF THE MEAN CURVATURE FLOW IN IMAGE FILTERING

The level set formulation of the mean curvature flow problem was suggested by Osher and Sethian in [13]. The corresponding nonlinear partial differential equation (PDE) has the following form

$$u_t - |\nabla u| \operatorname{div} \left( \frac{\nabla u}{|\nabla u|} \right) = 0, \quad (1)$$

where  $u(x, t)$  is an unknown level set function,  $(x, t) \in \Omega \times (0, T)$ ,  $\Omega \subset \mathbb{R}^d$  is an open bounded space domain (in image processing usually rectangular) and  $(0, T)$  is a time interval. The level set equation (1) is accompanied by an initial condition

$$u(x, 0) = u_0(x), x \in \Omega, \quad (2)$$

representing in image filtering a given noisy image, and by the boundary conditions which can be either zero Dirichlet or zero Neumann type. The mean curvature flow level set equation (1) and its generalizations have numerous applications in science, engineering and technology, ranging from free boundary problems in material sciences and computational fluid dynamics to filtering and segmentation algorithms in image processing and computer vision [15], [1]. In image processing applications, the equation (1) is called the curvature filter, it fulfills so-called morphological principle and represents an image smoothing by an intrinsic diffusion of image isophotes [1]. It has been generalized and used in various applications as edge enhancing image filtering [4], image segmentation by the geodesic active contours [3], [11] and by the (generalized) subjective surface methods [14], [5], [2]. Due to possibility of vanishing gradient

(corresponding to flat image areas) the equation (1) is in practice regularized by the Evans-Spruck approach [7] leading to equation

$$u_t - |\nabla u|_\varepsilon \operatorname{div} \left( \frac{\nabla u}{|\nabla u|_\varepsilon} \right) = 0, \quad (3)$$

where  $|\nabla u|_\varepsilon = \sqrt{|\nabla u|^2 + \varepsilon^2}$  and  $\varepsilon$  is a small regularization parameter.

The important analytical properties of the mean curvature flow such as a smoothing of image object boundaries (given by level sets of image intensity) in tangential direction only and a disappearing of small noisy spots due to their high curvature should be respected also by numerical schemes for solving (1) and its regularized version (3). Fulfilling such properties is related to non-diffusive behavior of a numerical scheme in direction normal to the image level sets.

There exist several approaches based on finite difference [13], [15], [12], finite element [6] and finite volume discretizations [10], [5], [9] of equation (3) which are used in practice and which has been studied also theoretically. The numerical analysis in this context is a nontrivial task due to nonlinear character and non-divergent form of (1) and (3). The numerical scheme presented in this paper was derived in [9] where stability and convergence of the numerical solution to a weak solution was proved considering more general nonlinear diffusion equations given in any open polyhedral subset  $\Omega$  of  $\mathbb{R}^d$ ,  $d \in \mathbb{N}$ , and for a general finite volume space discretization. In this paper we concentrate on application of the method in image processing, namely in image filtering by the mean curvature flow level set model. To that goal we present an efficient semi-implicit variant of the scheme on squared uniform grid corresponding to a pixel structure of an image. We compare our results with the widely used classical explicit finite difference scheme and show non-diffusive behavior of the new scheme in practical examples.

## II. STANDARD EXPLICIT FINITE DIFFERENCE SCHEME

First numerical method for solving mean curvature level set equation was proposed by Osher and Sethian in [13] and can be found e.g. in [15], Chapter 6. It became soon a standard due to its simplicity and straightforward computer implementation.

As an explicit scheme, it is not unconditionally stable and a relation between time step and grid size must be provided.

In two-dimensional case the equation (3) can be expressed in the following form

$$u_t - \frac{u_{xx}(u_y^2 + \varepsilon^2) + u_{yy}(u_x^2 + \varepsilon^2) - 2u_x u_y u_{xy}}{u_x^2 + u_y^2 + \varepsilon^2} = 0 \quad (4)$$

which is a basis for the numerical finite difference discretization. It uses forward Euler approximation of time derivative, second order central finite differences for the first and second order derivative terms.

Let  $\Omega$  be a rectangle in  $\mathbb{R}^2$  and  $T > 0$  be given. The discretization is done by dividing domain  $\Omega$  to a set of squares with the side of the length  $h$  and using uniform discrete time step  $\tau$ . We denote a vector of unknowns at the  $n$ -th time step by  $u_{i,j}^n$ , where the indices  $i = 1, \dots, N_1$ ,  $j = 1, \dots, N_2$  represent numbering of grid points (corresponding to pixel centers) in  $x$  and  $y$  direction. Let us denote

$$u_{x,i,j}^n = \frac{u_{i+1,j}^n - u_{i-1,j}^n}{2h}, \quad u_{y,i,j}^n = \frac{u_{i,j+1}^n - u_{i,j-1}^n}{2h},$$

$$u_{xx,i,j}^n = \frac{u_{i+1,j}^n - 2u_{i,j}^n + u_{i-1,j}^n}{h^2},$$

$$u_{yy,i,j}^n = \frac{u_{i+1,j}^n - 2u_{i,j}^n + u_{i-1,j}^n}{h^2},$$

$$u_{xy,i,j}^n = \frac{u_{i+1,j+1}^n + u_{i-1,j-1}^n - u_{i-1,j+1}^n - u_{i+1,j-1}^n}{4h^2},$$

and further

$$u_{x,i,j}^{n,\varepsilon} = (\varepsilon^2 + (u_{x,i,j}^n)^2), \quad u_{y,i,j}^{n,\varepsilon} = (\varepsilon^2 + (u_{y,i,j}^n)^2).$$

Then the explicit finite difference scheme for solving regularized mean curvature flow level set equation is given by

$$u_{i,j}^{n+1} = u_{i,j}^n + \tau \frac{u_{xx,i,j}^n u_{y,i,j}^{n,\varepsilon} + u_{yy,i,j}^n u_{x,i,j}^{n,\varepsilon} - 2u_{x,i,j}^n u_{y,i,j}^n u_{xy,i,j}^n}{\varepsilon^2 + (u_{x,i,j}^n)^2 + (u_{y,i,j}^n)^2}$$

### III. NEW FINITE VOLUME SCHEME

Unlike the finite difference scheme where the form of equation (4) is discretized, the finite volume method uses the basic form (3). Being semi-implicit, it is unconditionally stable. Its further advantage, in comparison with previous finite volume schemes [10], [5], is that not only solution values in centers of pixels but also the values at centers of pixel boundaries are used in discretization. Such approach allows a better approximation of gradients which is necessary for the problems like the level set equation (3). The finite volume scheme is derived in [9] and we present it here for the case of zero Dirichlet boundary condition. The case of Neumann zero boundary condition is straightforward.

Let  $\Omega$  be a rectangle in  $\mathbb{R}^2$ , such that there exists  $N_0, M_0 \in \mathbb{N}$  and  $h_0 > 0$  with  $\Omega = (0, N_0 h_0) \times (0, M_0 h_0)$ , and let  $T > 0$  be given.

We say that  $(\mathcal{D}, \tau)$ , with  $\mathcal{D} = (\mathcal{M}, \mathcal{E}, \mathcal{P})$ , is a space-time discretisation of  $\Omega \times (0, T)$  if there exist  $N_T \in \mathbb{N}$  with  $T = (N_T + 1)\tau$  and  $N, M \in \mathbb{N}$  and  $h > 0$  with  $\Omega = (0, Nh) \times (0, Mh)$ . We then define the following sets:

$$\mathcal{M} = \{ p_{i,j} = ((i-1)h, ih) \times ((j-1)h, jh), i = 1, \dots, N, j = 1, \dots, M \},$$

$$\begin{aligned} \mathcal{E} = & \{ \sigma_{i,j+\frac{1}{2}} = ((i-1)h, ih) \times \{jh\}, \\ & i = 1, \dots, N, j = 0, \dots, M \} \\ \cup & \{ \sigma_{i+\frac{1}{2},j} = \{ih\} \times ((j-1)h, jh), \\ & i = 0, \dots, N, j = 1, \dots, M \}, \end{aligned}$$

$\mathcal{E}_{\text{int}}$  (resp.  $\mathcal{E}_{\text{ext}}$ ) is the subset of all  $\sigma \in \mathcal{E}$  such that  $\sigma \subset \Omega$  (resp.  $\sigma \subset \partial\Omega$ ), for all  $p \in \mathcal{M}$ ,  $\mathcal{E}_p$  is the subset of all  $\sigma \in \mathcal{E}$  such that  $\sigma \subset \partial p$ ,  $\mathcal{N}_p$  is the subset of all  $q \in \mathcal{M}$  neighboring to  $p$ , and for all  $\sigma \in \mathcal{E}$ ,  $\mathcal{M}_\sigma$  is the subset of  $p \in \mathcal{M}$  such that  $\sigma \in \mathcal{E}_p$ ,

$$\mathcal{P} = \{ x_{i,j} = ((i-\frac{1}{2})h, (j-\frac{1}{2})h), \\ i = 1, \dots, N, j = 1, \dots, M \}.$$

Let  $(\mathcal{D}, \tau)$  be a space-time discretisation of  $\Omega \times (0, T)$ . We define the set  $H_{\mathcal{D}} \subset \mathbb{R}^{\mathcal{M}} \times \mathbb{R}^{\mathcal{E}}$  such that  $u_\sigma = 0$  for all  $\sigma \in \mathcal{E}_{\text{ext}}$ .

Let us define the approximation of initial condition by

$$u_p^0 = \frac{1}{|p|} \int_p u_0(x) dx, \quad \forall p \in \mathcal{M}, \quad (5)$$

and approximation of the gradient squared in finite volume by

$$N_p(u)^2 = \frac{2}{h^2} \sum_{\sigma \in \mathcal{E}_p} (u_\sigma - u_p)^2, \quad \forall p \in \mathcal{M}, \quad \forall u \in H_{\mathcal{D}} \quad (6)$$

and denote by

$$f_p^n = \sqrt{N_p(u^n)^2 + \varepsilon^2}. \quad (7)$$

Integrating equation (3) in every finite volume  $p$  and using divergence theorem [8] we obtain system of equations

$$\frac{h^2}{\tau} \frac{(u_p^{n+1} - u_p^n)}{f_p^n} - \frac{2}{f_p^n} \sum_{\sigma \in \mathcal{E}_p} (u_\sigma^{n+1} - u_p^{n+1}) = 0, \quad (8)$$

$$\forall p \in \mathcal{M}, \quad \forall n \in \mathbb{N},$$

where the following relation is given

$$\frac{u_\sigma^{n+1} - u_p^{n+1}}{f_p^n} + \frac{u_q^{n+1} - u_p^{n+1}}{f_q^n} = 0, \quad (9)$$

$\forall \sigma \in \mathcal{E}_{\text{int}}$  with  $\mathcal{M}_\sigma = \{p, q\}$ ,  $\forall n \in \mathbb{N}$ .

The following relation, deduced from (9),

$$u_\sigma^{n+1} = \frac{u_p^{n+1} f_q^n + u_q^{n+1} f_p^n}{f_p^n + f_q^n}, \quad (10)$$

and plugged in (8), provides the system of equations representing the semi-implicit scheme at the  $(n+1)$ -th time step:

$$\begin{aligned} & \frac{h^2}{\tau} \frac{u_p^{n+1}}{f_p^n} + \sum_{q \in \mathcal{N}_p} 2 \frac{u_p^{n+1} - u_q^{n+1}}{f_p^n + f_q^n} \\ & + \sum_{\sigma \in \mathcal{E}_p \cap \mathcal{E}_{\text{ext}}} 2 \frac{u_p^{n+1}}{f_p^n} = \frac{h^2}{\tau} \frac{u_p^n}{f_p^n}. \end{aligned} \quad (11)$$

Let us develop the system of equations issued from (11), denoting for short  $u_{i,j}^n$  instead of  $u_{p_{i,j}}^n$ ,  $u_{i+\frac{1}{2},j}^n$  instead of  $u_{\sigma_{i+\frac{1}{2},j}}^n$  and  $u_{i,j+\frac{1}{2}}^n$  instead of  $u_{\sigma_{i,j+\frac{1}{2}}}^n$ . First, the values  $u_{i,j}^0$ ,  $u_{i+\frac{1}{2},j}^0$ , and  $u_{i,j+\frac{1}{2}}^0$  are computed from the initial condition, namely  $u_{i,j}^0$  is given by the value of initial condition at point  $x_{i,j}$ ,  $u_{i,j+\frac{1}{2}}^0$  at point  $((i - \frac{1}{2})h, jh)$  and  $u_{i+\frac{1}{2},j}^0$  at point  $(ih, (j - \frac{1}{2})h)$ .

Then in every discrete time step  $n+1$ ,  $n = 0, \dots$  we compute  $N_p(u^n)$  which is present in  $f_p^n$  and form the linear system to be solved. To that goal we compute, in accordance with (6),

$$2(N_{i,j}^n)^2 = \left( \frac{u_{i,j}^n - u_{i,j+\frac{1}{2}}^n}{\frac{h}{2}} \right)^2 + \left( \frac{u_{i,j}^n - u_{i+\frac{1}{2},j}^n}{\frac{h}{2}} \right)^2 + \left( \frac{u_{i,j}^n - u_{i,j-\frac{1}{2}}^n}{\frac{h}{2}} \right)^2 + \left( \frac{u_{i,j}^n - u_{i-\frac{1}{2},j}^n}{\frac{h}{2}} \right)^2,$$

and its regularization is computed by

$$f_{i,j}^n = \sqrt{(N_{i,j}^n)^2 + \varepsilon^2}.$$

Then we can construct coefficients of the linear system (11) (taking the example of a control volumes which has no edges at the boundary of the domain) by the formulas

$$\begin{aligned} a_{i+\frac{1}{2},j} &= \frac{2}{f_{i,j}^n + f_{i+1,j}^n}, \quad a_{i,j+\frac{1}{2}} = \frac{2}{f_{i,j}^n + f_{i,j+1}^n}, \\ a_{i,j} &= a_{i+\frac{1}{2},j} + a_{i-\frac{1}{2},j} + a_{i,j+\frac{1}{2}} + a_{i,j-\frac{1}{2}} + \frac{h^2}{\tau} \frac{1}{f_{i,j}^n}, \\ b_{i,j} &= \frac{h^2}{\tau} \frac{u_{i,j}^{n-1}}{f_{i,j}^n} \end{aligned}$$

and solve the linear system

$$\begin{aligned} a_{i,j}u_{i,j} - a_{i+\frac{1}{2},j}u_{i+1,j} - a_{i-\frac{1}{2},j}u_{i-1,j} \\ - a_{i,j-\frac{1}{2}}u_{i,j-1} - a_{i,j+\frac{1}{2}}u_{i,j+1} = b_{i,j}, \end{aligned} \quad (12)$$

e.g. by the successive-over-relaxation (SOR) iterative linear solver in order to obtain the solution  $u_{i,j}^{n+1}$  at the new time step. Finally from the relation (10) we compute  $u_{i\pm\frac{1}{2},j}^{n+1}$  and  $u_{i,j\pm\frac{1}{2}}^{n+1}$  by the formulas

$$\begin{aligned} u_{i-\frac{1}{2},j}^{n+1} &= \frac{f_{i,j}^n u_{i-1,j}^{n+1} + f_{i-1,j}^n u_{i,j}^{n+1}}{f_{i,j}^n + f_{i-1,j}^n}, \\ u_{i,j-\frac{1}{2}}^{n+1} &= \frac{f_{i,j}^n u_{i,j-1}^{n+1} + f_{i,j-1}^n u_{i,j}^{n+1}}{f_{i,j}^n + f_{i,j-1}^n}. \end{aligned}$$

**Lemma ( $L^\infty$  stability of the scheme)** We denote by

$$|u_0|_{\mathcal{D},\infty} = \max_{p \in \mathcal{M}} |u_p^0|, \quad (13)$$

(note that, if  $u_0 \in L^\infty(\Omega)$  then  $|u_0|_{\mathcal{D},\infty} \leq \|u_0\|_{L^\infty(\Omega)}$ ). Let  $(u_p^n)_{p \in \mathcal{M}, n \in \mathbb{N}}$  be a solution of (8), (9). Then it holds:

$$|u_p^n| \leq |u_0|_{\mathcal{D},\infty} \forall p \in \mathcal{M}, \forall n = 0, \dots, N_T.$$

**Proof.** Suppose that for fixed time step  $(n+1)$  the maximum of all  $u_p^{n+1}$  is achieved at the finite volume  $p$ . Let us write (8) in the following way:

$$u_p^{n+1} + \frac{\tau}{h^2} \sum_{\sigma \in \mathcal{E}_p} 2(u_p^{n+1} - u_\sigma^{n+1}) = u_p^n, \quad (14)$$

Since the value  $u_\sigma^{n+1}$  satisfies the equality (9) which is a convex linear combination of values  $u_p^{n+1}$ ,  $u_q^{n+1}$ , we obtain

$$u_p^{n+1} - u_\sigma^{n+1} = \frac{f_p^n(u_p^{n+1} - u_q^{n+1})}{f_p^n + f_q^n},$$

which is nonnegative. This leads to

$$u_p^{n+1} \leq u_p^n. \quad (15)$$

Then, we recursively get the estimate (15), similarly reasoning for the minimum values.

#### IV. COMPARISON OF THE SCHEMES IN IMAGE FILTERING

In this section we present comparison of the schemes in artificially noised examples and in real image processing tasks related to filtering of two-photon laser scanning biological images. For the semi-implicit finite volume scheme we use natural relation  $\tau = h^2$  between space and time step, where  $h = 1/N_1$  is the length of space step (pixel size). Due to stability reasons we had to impose  $\tau = h^2/4$  for the explicit finite difference scheme in these examples.

##### Example 1.

In this example, we consider an image containing black cinquefoil on white background deteriorated by a 20 % salt-and-pepper noise. Dimensions of the image are  $N_1 = N_2 = 200$ . Figure 1 shows the results of the filtering by the semi-implicit finite volume scheme compared with the result of the explicit finite difference scheme. One can observe that the black cinquefoil is satisfactory reconstructed by the finite volume scheme, while diffused image as a filtering result can be seen for the explicit finite difference scheme. In Figure 2 one can see isolines of images filtered by both schemes in the last time step. The isolines in the result of the finite volume scheme are all concentrated along the edge, while the isolines in the result by the explicit finite difference scheme are spread, especially in the central image part.

##### Example 2.

Now we consider an image with black quatrefoil on white background endowed by a 50 % salt-and-pepper noise. Dimensions of the image are  $N_1 = N_2 = 200$ . Figure 3 shows the results of filtering by the semi-implicit finite volume scheme compared with the result of the explicit finite difference scheme. Again, the black quatrefoil is satisfactorily reconstructed by the finite volume scheme in a few computational time steps, while with this level of noise it cannot be correctly filtered by a more diffusive explicit finite difference scheme.

##### Example 3.

Image used in this example contains black asteroid on white background deteriorated again by a 50 % salt-and-pepper noise. Dimensions of the image are  $N_1 = N_2 = 400$ . In Figure 4 we can see again non-diffusive filtering results by

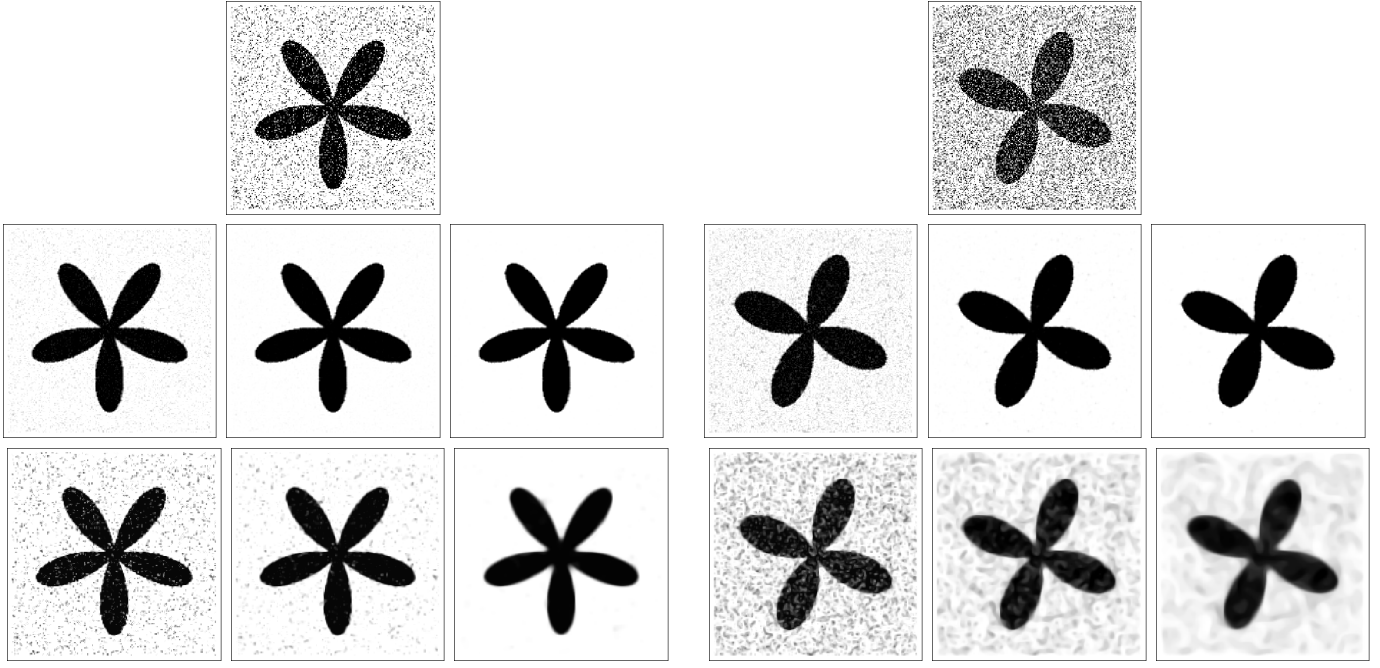


Fig. 1. Example 1, initial image with 20 % salt-and-pepper noise (top), filtering by the semi-implicit finite volume scheme after 1 (middle left), 2 (middle middle) and 3 (middle right) time steps, and filtering by the explicit finite difference scheme after 1 (bottom left), 4 (bottom middle) and 30 (bottom right) time steps.

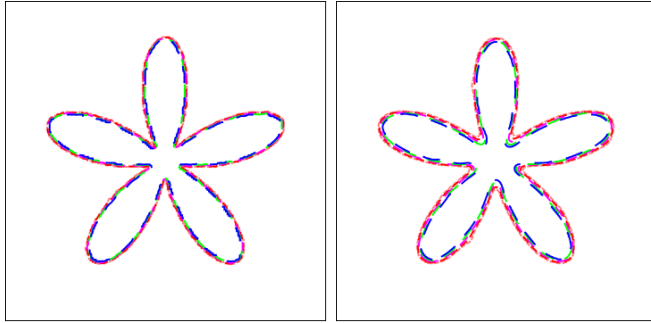


Fig. 2. Example 1, izolines for values 0.1 (pink) 0.3 (red) 0.5 (magenta), 0.7 (green), 0.9 (blue) of the filtering results by the semi-implicit FV scheme after 4 time steps (left) and by the explicit FD scheme after 30 time steps (right).

the semi-implicit finite volume scheme compared with the results of the explicit finite difference scheme. In Figure 5 you can see izolines of images filtered by both schemes in the last time step. The finite difference scheme does not keep corners and for this level of noise spurious structures outside of astroid appear. Further continuation of the filtering process would cause more uniform background outside the astroid but also strong smoothing and blurring of the astroid shape.

In the following examples we present filtering of real images which come from two-photon laser scanning microscopy. They represent 2D slices of 3D images of cell membranes and nuclei chosen from 3D image sequences representing acquisition of

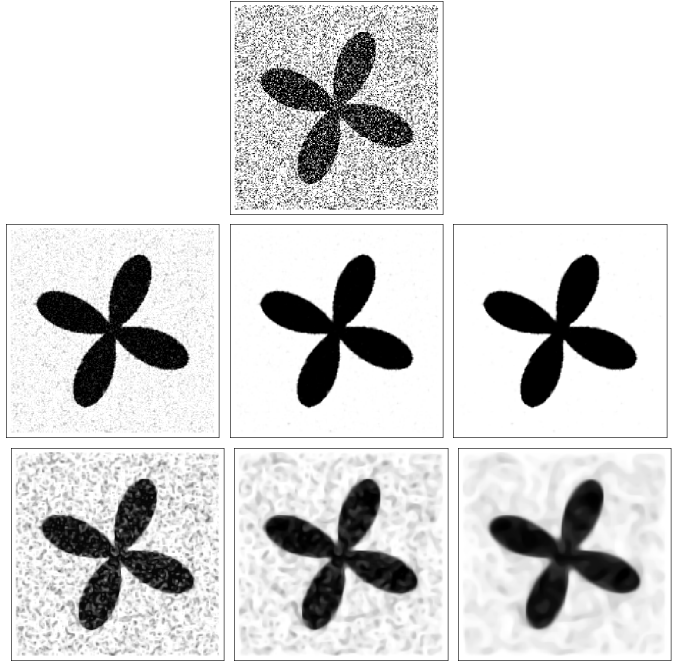


Fig. 3. Example 2, the initial image with 50 % salt-and-pepper noise (top), filtering by the semi-implicit FV scheme after 1 (middle left), 3 (middle middle) and 4 time steps (middle right), and filtering by the explicit FD scheme after 4 (bottom left), 16 (bottom middle), and 50 (bottom right) time steps.

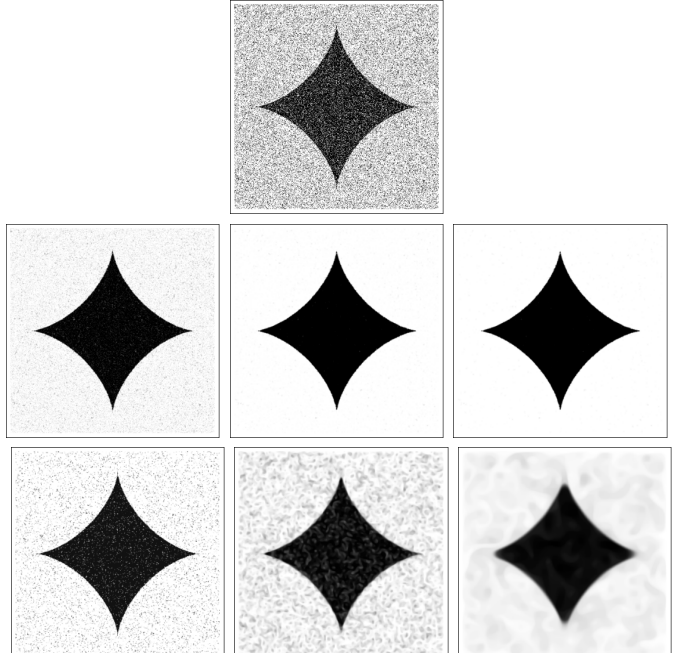


Fig. 4. Example 3, the initial image with 50 % salt-and-pepper noise (top), filtering results by the semi-implicit FV scheme after 1 (middle left), 3 (middle middle) and 4 (middle right) time steps, and filtering by the explicit FD scheme after 4 (bottom left), 16 (bottom middle), and 200 (bottom right) time steps.

early stages of zebrafish embryogenesis.

#### Example 4.

The original image represents cell membranes with high-

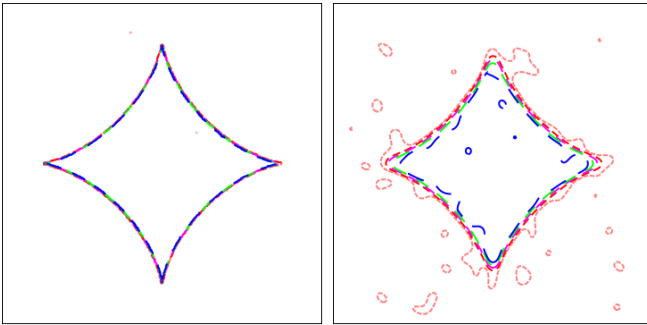


Fig. 5. Example 3, izolines for values 0.1 (pink) 0.3 (red) 0.5 (magenta), 0.7 (green), 0.9 (blue) of the filtering results by the semi-implicit FV scheme after 4 time steps (left) and by the explicit FD scheme after 200 time steps (right).

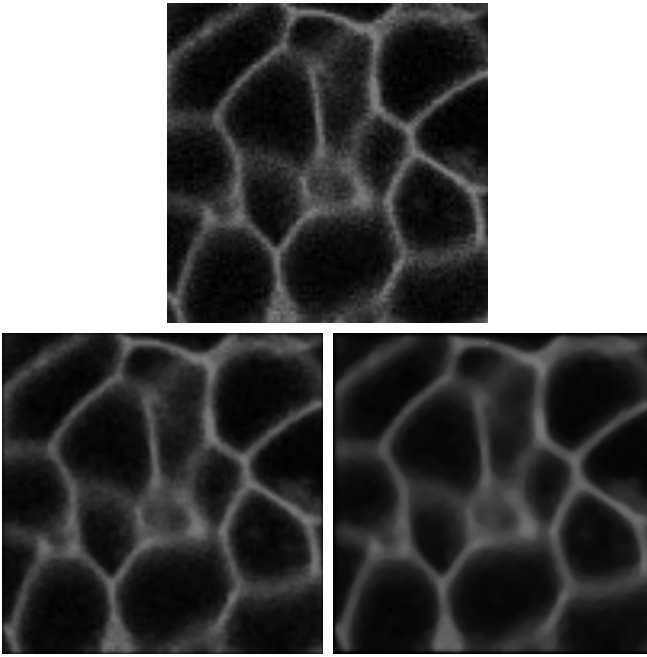


Fig. 6. Example 4, the initial noisy image of cell membranes (top). Filtering by the semi-implicit FV scheme after 1 (bottom left) and 5 (bottom right) time steps ( $\tau = h^2$ ).

level of noise included. The image size is  $200 \times 200$  pixels. One can observe in Figure 6 that mean curvature flow type filtering diffuses the image along the intensity isolines and thus it improves the connectivity of the coherent structures as cell borders.

In Figures 7 and 8 we show an edge detection of unfiltered image together with edge detection of filtering results by semi-implicit finite volume scheme (Fig. 7) and explicit finite difference scheme (Fig. 8). As one can see, the edge detection is slightly more sharp for the finite volume scheme which is a consequence of its less diffusive behaviour.

#### Example 5.

The image in this example represents cell nuclei which, although disconnected, forms observable morphogenetic structures appearing during embryogenesis. The mean curvature flow type filtering, since diffusing in tangential direction only,

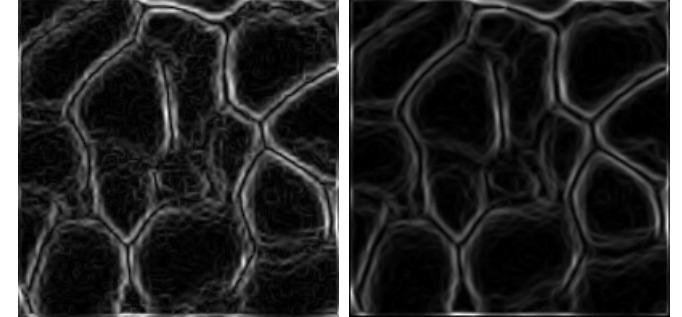
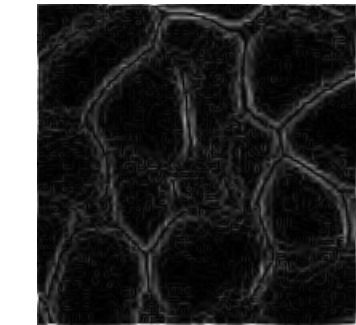


Fig. 7. Example 4, an edge detection of the initial noisy image of cell membranes (top), and an edge detection of the filtering results obtained by the semi-implicit FV scheme after 1 (bottom left) and 5 (bottom right) time steps ( $\tau = h^2$ ).

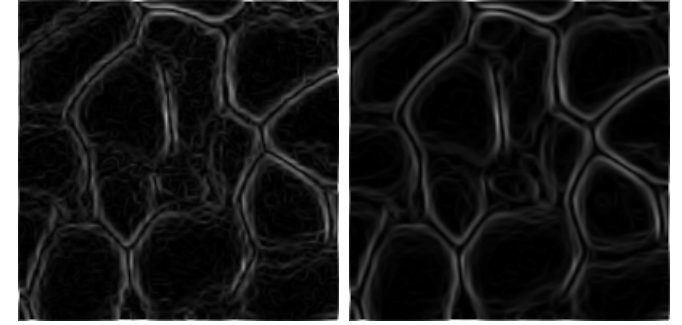


Fig. 8. Example 4, an edge detection of the filtering results obtained by the explicit finite difference scheme after 4 (left) and 20 (right) time steps ( $\tau = \frac{h^2}{4}$ ).

again improves the coherency of structure borders as can be seen in Figure 9. The image size is  $300 \times 300$  pixels.

## V. CONCLUSION

In this paper we have shown non-diffusive behaviour of the new numerical scheme based on semi-implicit finite volume discretization of the mean curvature flow level set equation. The comparison with the standard explicit finite difference scheme shows its capability of high quality image and shape reconstruction also in case of high level of noise. It is shown on representative examples that new finite volume scheme much better keeps desired theoretical properties of mean curvature flow filtering which should diffuse an image in tangential direction to level sets only and filter out the noisy spots very quickly. The results were presented both on artificially noised images and on real images coming from two-photon laser

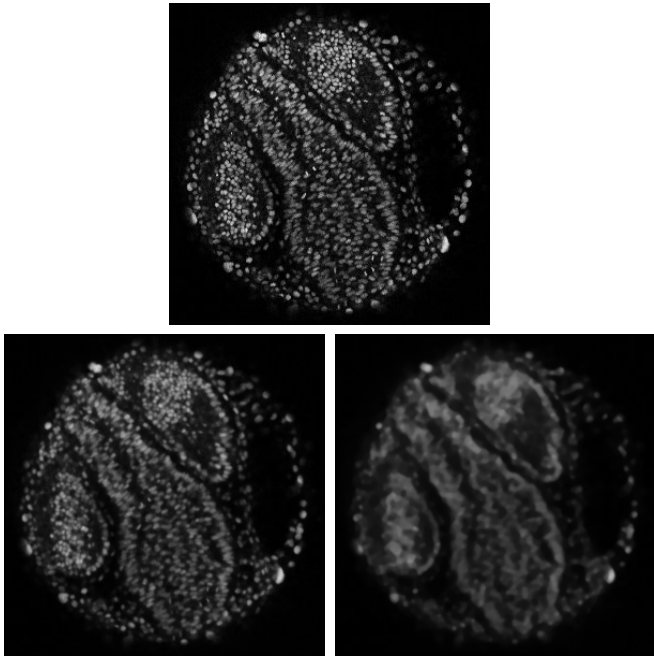


Fig. 9. Example 5, the initial noisy image of cell nuclei (top). Filtering results by the semi implicit FV scheme after 1 (bottom left) and 5 (bottom right) time steps,  $\tau = h^2$ .

microscope acquisition of early stages of zebrafish embryogenesis.

#### ACKNOWLEDGMENT

The authors would like to thank Dr. Nadine Peyriéras from CNRS, Gif sur Ivette, for embryogenesis testing data. The work of second and third author was supported by grants APVV-0351-07 and VEGA 1/0269/09, 1/0733/10.

#### REFERENCES

- [1] L. Alvarez, F. Guichard, P. L. Lions and J. M. Morel, *Axioms and fundamental equations of image processing*, Arch. Rational Mech. Anal., 123(3):199–257, 1993.
- [2] P. Bourgine, R. Čunderlík, O. Drblíková, K. Mikula, N. Peyriéras, M. Remešíková, A. Sarti, and B. Rizzi, *4d embryogenesis image analysis using pde methods of image processing*, to appear in Kybernetika, 2010.
- [3] V. Caselles, R. Kimmel and G. Sapiro, *Geodesic active contours*. International Journal of Computer Vision, 22(1):61–79, 1997.
- [4] Y. Chen, B. C. Vemuri, and L. Wang, *Image denoising and segmentation via nonlinear diffusion*, Comput. Math. Appl., 39(5-6):131–149, 2000.
- [5] S. Corsaro, K. Mikula, A. Sarti, and F. Sgallari, *Semi-implicit covolume method in 3D image segmentation*, SIAM J. Sci. Comput., 28(6):2248–2265, 2006.
- [6] K. Deckelnick and G. Dziuk, *Error estimates for a semi-implicit fully discrete finite element scheme for the mean curvature flow of graphs*, Interfaces Free Bound., 2(4):341–359, 2000.
- [7] L. C. Evans and J. Spruck, *Motion of level sets by mean curvature I*, J. Differ. Geom., 33(3):635–681, 1991.
- [8] R. Eymard, T. Gallouët, and R. Herbin, *Finite volume methods*, Ciarlet, P. G. (ed.) et al., Handbook of numerical analysis. Vol. 7: Solution of equations in  $\mathbb{R}^n$  (Part 3). Techniques of scientific computing (Part 3). Amsterdam: North-Holland/ Elsevier, 713-1020 (2000), 2000.
- [9] R. Eymard, A. Handlovicová and K. Mikula, *Study of a finite volume scheme for the regularised mean curvature flow level set equation*, submitted to IMA J. Numerical Analysis (<http://www.math.sk/mikula/publications.html>)
- [10] A. Handlovicová, K. Mikula and F. Sgallari, *Semi-implicit complementary volume scheme for solving level set like equations in image processing and curve evolution*, Numer. Math., 93 (4): 675–695, 2003
- [11] S. Kichenassamy, A. Kumar, P. Olver, A. Tannenbaum, and A. jun. Yezzi, *Conformal curvature flows: from phase transitions to active vision*. Arch. Ration. Mech. Anal., 134(3):275–301, 1996.
- [12] A. M. Oberman, *A convergent monotone difference scheme for motion of level sets by mean curvature*. Numer. Math., 99(2):365–379, 2004.
- [13] S. Osher and J. A. Sethian, *Fronts propagating with curvature-dependent speed: Algorithms based on Hamilton-Jacobi formulations*. J. Comput. Phys., 79(1):12–49, 1988.
- [14] A. Sarti, R. Malladi, and J. A. Sethian, *Subjective surfaces: A method for completing missing boundaries*. Proc. Natl. Acad. Sci. USA, 97(12):6258–6263, 2000.
- [15] J. A. Sethian, *Level set methods and fast marching methods. Evolving interfaces in computational geometry, fluid mechanics, computer vision, and materials science.*, Cambridge Monographs on Applied and Computational Mathematics. 3. Cambridge: Cambridge University Press, 378 p., 1999.